Topological and chemical ordering in $Co_{43}Fe_{20}Ta_{5.5}B_{31.5}$ metallic glass

Ivan Kaban,[1,*] Pál Jóvári,[2] Mihai Stoica,[3] Jürgen Eckert,[3,†] Walter Hoyer,[1] and Brigitte Beuneu[4]
[1]*Institute of Physics, Chemnitz University of Technology, D-09107 Chemnitz, Germany*
[2]*Research Institute for Solid State Physics and Optics, H-1525 Budapest, POB 49, Hungary*
[3]*IFW Dresden, Institute for Complex Materials, P.O. Box 27 01 16, D-01171 Dresden, Germany*
[4]*Laboratoire Léon Brillouin, CEA, Saclay 91191 Gif sur Yvette Cedex, France*
(Received 23 February 2009; revised manuscript received 22 April 2009; published 18 June 2009)

Atomic structure of $Co_{43}Fe_{20}Ta_{5.5}B_{31.5}$ metallic glass has been studied with x-ray and neutron diffraction, extended x-ray absorption fine structure experiments, and reverse Monte Carlo modeling. Each boron atom is found to have an average 2.3 nearest boron neighbors, which is significantly higher than in binary $Co_{81.5}B_{18.5}$ and $Fe_{80}B_{20}$ glasses. The existence of Ta-based structural units with the composition close to the stoichiometry of the $(Co,Fe)_{21}Ta_2B_6$ crystalline phase precipitating upon annealing of the glass is established. Ta-B and B-B bonds, which are absent in the crystalline state, are suggested to be responsible for the high glass-forming ability and thermal stability of the $Co_{43}Fe_{20}Ta_{5.5}B_{31.5}$ glass.

DOI: 10.1103/PhysRevB.79.212201 PACS number(s): 61.43.Dq, 61.05.cj, 61.05.cp, 61.05.fm

Cobalt- and iron-based metallic glasses (MG) exhibit exceptional structural and functional properties that promise practical applications in various fields such as surface coatings, cutting tools, sensors, or memories.[1] In 2003, Inoue *et al.*[2,3] reported the best glass-forming ability (GFA) of the $Co_{43}Fe_{20}Ta_{5.5}B_{31.5}$ alloy (CoFeTaB) in the Co-Fe-based alloy family. Bulk CoFeTaB glass exhibited the highest fracture strength and Young's modulus among all known crystalline and glassy metallic alloys.[2–4] Moreover, glassy $Co_{43}Fe_{20}Ta_{5.5}B_{31.5}$ is characterized by excellent soft magnetic properties and high corrosion resistance.[5] All this rises the scientific and technological interest in this material and prompts investigation of their physical basis. Atomic structure of the CoFeTaB glass has not been revealed so far.

In this Brief report, we report the data on the topological and chemical atomic ordering in the $Co_{43}Fe_{20}Ta_{5.5}B_{31.5}$ glass obtained by a complex study that includes x-ray diffraction (XRD), neutron diffraction (ND), extended x-ray absorption fine structure (EXAFS) measurements and the reverse Monte Carlo (RMC) modeling. It has been shown in some recent works[6–9] that the local atomic structure of multicomponent noncrystalline alloys can be studied successfully if multiple experimental data sets are modeled simultaneously with the help of RMC technique. Often, combination of XRD and ND data for a binary alloy is enough to produce reliable partial pair distribution functions $g_{ij}(r)$.[6] In some binary alloys, EXAFS data are very useful as they are element specific and determine the interactomic distances with a high accuracy.[7] In ternary glasses, only combination of two diffraction curves and EXAFS information can separate the six partial distributions.[8,9] In the case of four-component CoFeTaB glass, where ten $g_{ij}(r)$ functions have to be resolved, as many experimental data as possible should be applied.

A master alloy with nominal composition $Co_{43}Fe_{20}Ta_{5.5}B_{31.5}$ was prepared by arc melting of pure Co (99.9%), Fe (99.95%), Ta (99.96%), and B (99.5%) under a Ti-gettered Ar atmosphere. Amorphous ribbons (width of 4 mm, thickness of ~ 20 μm) were obtained by single-roller melt spinning on a copper wheel under Ar flow at 24 ms^{-1} tangential wheel velocity. XRD experiments were carried out at the BW5 beamline at HASYLAB (DESY, Hamburg, Germany) with the energy of the incident beam of 99.8 keV. ND measurements were carried out with the 7C2 diffractometer at the LLB (CEA-Saclay, France). The wavelength of the incident radiation was 0.73 Å. Due to natural B, the absorption of the sample was high. To optimize the signal-to-noise ratio, the sample was loaded into an annular sample holder (internal diameter: 8 mm, external diameter: 10 mm). The EXAFS measurements at the Co and Fe *K*-absorption edges and at the Ta L_I-absorption edge were carried out at the HASYLAB beamline X1 in transmission mode using fixed exit double-crystal Si(111). Details on the data treatment can be found elsewhere.[7] The experimental XRD and ND structure factors as well as k^3 weighted EXAFS $\chi(k)$ curves are shown in Fig. 1.

Details of the RMC technique and its application can be found in Refs. 6–11. In the present work, the five experimental data sets were modeled simultaneously by the RMC. The simulation box contained 24 000 atoms. The number density of the system (0.1045 $Å^{-3}$) was calculated from the mass density of the $Co_{43}Fe_{20}Ta_{5.5}B_{31.5}$ MG (8.65 g/cm^3).[2] The minimum interatomic distances (cutoffs) applied: 1.8 Å for Co-B, Fe-B and B-B; 2.0 Å for B-Ta and Fe-Fe; 2.1 Å for Co-Co and Co-Fe; 2.2 Å for Co-Ta and Fe-Ta; and 3.5 Å for Ta-Ta. The final simulation run consisted of $2 \cdot 10^7$ accepted single atomic moves and about 500 000 successful swap moves. The model curves are compared with the experimental data in Fig. 1, while the partial pair distribution functions $g_{ij}(r)$ are plotted in Fig. 2. The mean nearest-neighbor distances r_{ij} and coordination numbers N_{ij} obtained by the simultaneous fit of all data sets are summarized in Table I. The error of r_{ij} is about 0.02 Å. The uncertainty of N_{ij} is about 10% for Fe/Co-Fe/Co and 20% for the remaining pairs.

Several test runs were carried out with various data sets to learn more about the interplay of data and constraints. The results of these can be summarized in the following: (i) with the above cutoffs, the XRD measurement alone can separate Fe/Co-Fe/Co and Fe/Co-Ta correlations; (ii) by introducing Fe and Co *K*-edge EXAFS data, Co-Ta and Fe-Ta distances are resolved. Adding the Ta L_1 data set does not significantly change the Co-Ta and Fe-Ta parameters but sharpens the first peak of $g_{TaB}(r)$, which has a very low contribution to diffraction data; (iii) if modeling is carried out without the ND

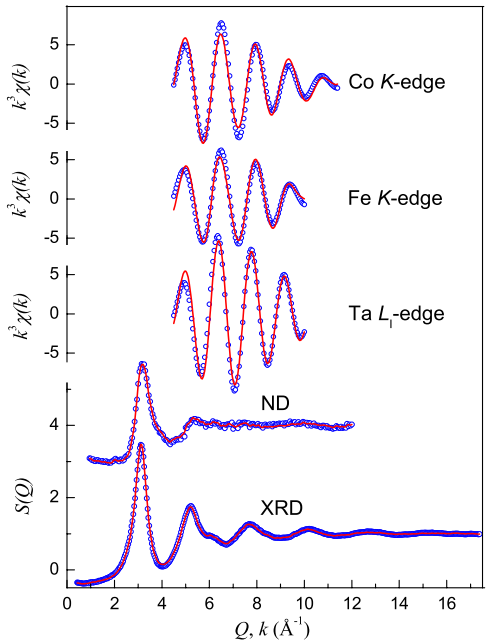

FIG. 1. (Color online) XRD and ND structure factors and EXAFS spectra for $Co_{43}Fe_{20}Ta_{5.5}B_{31.5}$ metallic glass: *circles*–experimental data, *lines*–obtained by simultaneous RMC modeling of five measurements.

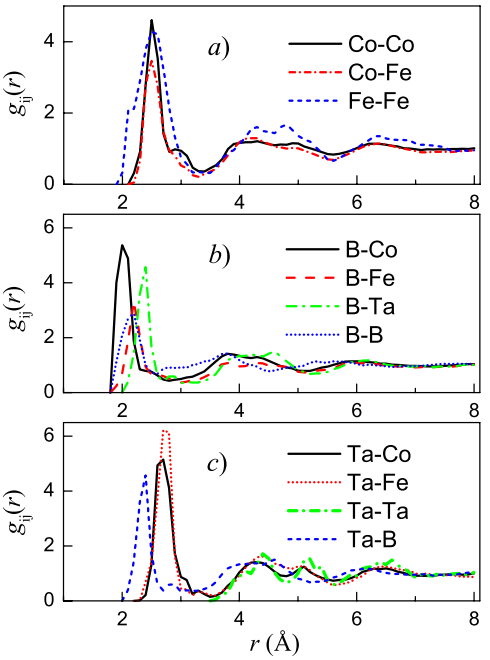

FIG. 2. (Color online) Partial pair distribution functions for $Co_{43}Fe_{20}Ta_{5.5}B_{31.5}$ metallic glass extracted from the RMC final 3D configuration box.

structure factor then the B-B peak distance is determined by the B-B cutoff constraint. Thus, ND data are absolutely necessary to get a reliable estimate of B-B distance and coordination number. Examples of different runs are demonstrated in Fig. 3.

Despite many similarities of Co and Fe[12] there is a remarkable difference between their coordination environments in the CoFeTaB glass [Fig. 2(a)], which undoubtedly stem from the experimental data as the simulation runs started from random configurations with the same cutoff values for both elements. The coordination of Co and Fe atoms is virtually the same if only metal neighbors (Co, Fe, Ta) are considered. On the average: (i) one Co atom has 9.6 ± 0.5 Co/Fe and 1.0 ± 0.2 Ta neighbors; (ii) one Fe atom has 10.2 ± 0.5 Co/Fe and 1.1 ± 0.2 Ta neighbors. However, the average Co-B coordination number (3.7 ± 0.7) is significantly higher than the Fe-B coordination number (2.3 ± 0.5).

Partial pair distribution functions describing the environ-

TABLE I. Mean nearest-neighbor distances r_{ij} and coordination numbers N_{ij} for $Co_{43}Fe_{20}Ta_{5.5}B_{31.5}$ metallic glass. The values for $Co_{81.5}B_{18.5}$ and $Fe_{80}B_{20}$ binary glasses are also given for comparison. The error of r_{ij} is about 0.02 Å. The uncertainty of N_{ij} is about 10% for Fe/Co-Fe/Co and 20% for the remaining pairs.

	$Co_{43}Fe_{20}Ta_{5.5}B_{31.5}$ [b]		$Co_{81.5}B_{18.5}$ [b]		$Co_{81.5}B_{18.5}$ [c]		$Fe_{80}B_{20}$ [c]	
Pairs i,j	r_{ij} (Å)	N_{ij}/N_{ji}	r_{ij} (Å)	N_{ij}/N_{ji}	r_{ij} (Å)	N_{ij}/N_{ji}	r_{ij} (Å)	N_{ij}/N_{ji}
Co-Co	2.52	7.0	2.49	11.2	2.50	12.7		
Co-Fe/Fe-Co	2.51	2.6/5.6						
Co-Ta/Ta-Co	2.69	1.0/8.1						
Co-B/B-Co	2.02	3.7/5.1	2.07	1.9/8.2	2.07	1.5/6.6		
Fe-Fe	2.51	4.6					2.55	11.5
Fe-Ta/Ta-Fe	2.73	1.1/4.0						
Fe-B/B-Fe	2.20	2.3/1.5					2.13	2.2/8.9
Ta-Ta[a]		0						
Ta-B/B-Ta	2.37	2.9/0.5						
B-B	2.15	2.3	2.09	0.6				

[a]Ta-Ta nearest neighbors were eliminated by setting the Ta-Ta cutoff to 3.5 Å.
[b]This work.
[c]Reference 25

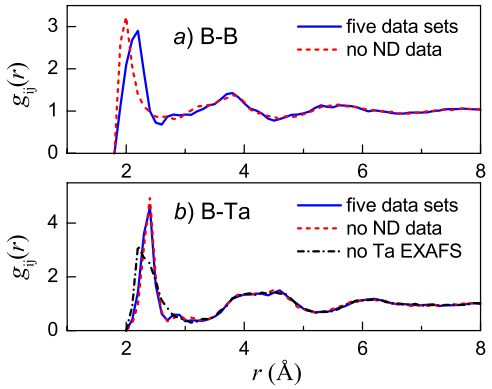

FIG. 3. (Color online) B-B (a) and B-Ta (b) partial pair distributions extracted from the atomic configurations modeled using different input data sets: *five data sets*–XRD, ND and Co-, Fe-, Ta-EXAFS; *no ND data*–XRD and Co-, Fe-, Ta-EXAFS; *no Ta EXAFS*–XRD, ND and Co-, Fe-EXAFS.

ment of boron $g_{BX}(r)$ are well resolved [Fig. 2(b)]. The B-Co interatomic distance (r_{BCo}=2.02 Å) is shorter suggesting that the bond is stronger than B-Fe bond (r_{BFe}=2.20 Å). The ratio of the B-Co and B-Fe average coordination numbers (N_{BCo}/N_{BFe}=5.1/1.5≈3.4) is significantly higher than the ratio of Co and Fe concentrations in the alloy (0.43/0.20 =2.15), which means that B prefers Co rather than Fe neighbors. It is noteworthy that the average B-B coordination number is ~2.3.

The presence of direct B-B contacts in Co-B, Fe-B, and Ni-B metallic glasses has always been discussed with a great caution (see for example Refs. 23 and 25, and citations therein). The main problem is the very small B-B contribution to the experimental diffraction curves, which makes the separation of $g_{BB}(r)$ extremely difficult. Pusztai and Sváb[11] applied RMC simulation to the $Ni_{65}B_{35}$ glass with rather high B content and showed the existence of B-B pairs (N_{BB}≈1 was found). The formation of short boron chains in the glassy $Ni_{65}B_{35}$ was supposed to be possible.

We performed RMC modeling of the $Co_{81.5}B_{18.5}$ and $Fe_{80}B_{20}$ glasses using the XRD and ND structure factors of Lamparter *et al.*[13] both with and without B-B bonding. It was not possible to get physically reasonable B-B partial pair distribution function neither for Co-B nor for Fe-B glasses if the closest B-B approach was set at 3.0 Å. If the B-B minimum distance is decreased down to 1.8 Å, the pair distribution function $g_{BB}(r)$ for the binary MGs bears a strong resemblance to the same function of the CoFeTaB glass as it is illustrated in Fig. 4. In spite of the similarity of the B-B pair distribution function in Co-B and CoFeTaB glasses, N_{BB} in the binary alloy is only about 0.6, which is significantly smaller than in the quaternary alloy (N_{BB}≈2.3). A similar scenario is suggested from the analysis of literature data on $Fe_{80}B_{20}$;[13] however, a reliable resolution of Fe-B and B-B is not possible on the basis of the existing experimental data due to the very low contribution of B-B correlations both to the ND and XRD curves. Table I lists r_{ij} and N_{ij} for the $Co_{81.5}B_{18.5}$ and $Fe_{80}B_{20}$ glasses reported by Lamparter *et al.*[13] as well as the values obtained by us. Despite the very close atomic radii of Co(1.26 Å) and Fe(1.25 Å),[12] the difference in r_{CoB} and r_{FeB} is 0.06 Å in the binary glasses[13] and it is remarkably larger in the CoFeTaB glass (0.18 Å). It is noteworthy that boron-boron coordination number increases from $N_{BB}<1$ in the $Fe_{80}B_{20}$ and $Co_{81.5}B_{18.5}$ glasses up to N_{BB}≈2.3 in the $Co_{43}Fe_{20}Ta_{5.5}B_{31.5}$. This suggests that boron atoms build a network throughout the $Co_{43}Fe_{20}Ta_{5.5}B_{31.5}$ glass.

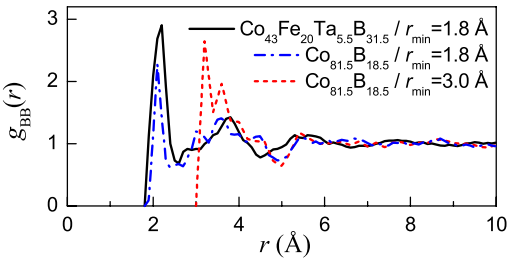

FIG. 4. (Color online) Boron-boron partial pair distribution function in $Co_{43}Fe_{20}Ta_{5.5}B_{31.5}$ and $Co_{81.5}B_{18.5}$ glasses with various B-B cutoff r_{min}.

Because of the low-Ta concentration, the experimental data are not sensitive to Ta-Ta correlations. It was assumed that there are no Ta-Ta nearest neighbors and the cutoff was raised to 3.5 Å. The positions of the first peak on $g_{TaCo}(r)$, $g_{TaFe}(r)$, and $g_{TaB}(r)$ are much larger than the respective cutoffs used in the modeling, which clearly indicates that they are determined by the experimental data [Fig. 2(c)]. The mean interatomic distances Ta-Co (2.69 Å) and Ta-Fe (2.73 Å) in the CoFeTaB glass are close to each other. On the average, one Ta atom has 8.1±1.6 Co, 4.0±0.8 Fe, and 2.9±0.6 B neighbors. It is interesting that with these values the average composition of the first-coordination shell including the central Ta atom is $(Co,Fe)_{75.6}Ta_{6.3}B_{18.1}$. This composition is different from the actual composition of the glassy alloy studied but is very close to that of the crystalline phase $(Co,Fe)_{21}Ta_2B_6$ precipitating upon annealing of the $Co_{43}Fe_{20}Ta_{5.5}B_{31.5}$ glass at 928 K, that is 18 K above T_g.[3] It can be assumed that due to the proper stoichiometry of Ta-based structural units, the $(Co,Fe)_{21}Ta_2B_6$ phase nucleates at these units upon thermal treatment.

A remarkable feature of glassy $Co_{43}Fe_{20}Ta_{5.5}B_{31.5}$ is the presence of Ta-B (r_{TaB}=2.37 Å) and B-B bonds (r_{BB} =2.15 Å) which are absent in the crystalline $(Co,Fe)_{21}Ta_2B_6$ phase[14] with the structure of the ternary τ-boride $Co_{21}Ta_2B_6$.[15] Metalloid-metalloid bonds are also absent in the analogous binary carbide $Cr_{23}C_6$.[16] The closest Ta-B and B-B distances in the crystalline $(Co,Fe)_{21}Ta_2B_6$ are 3.737 Å and 3.417 Å, respectively. Figure 5 illustrates the distribution of Ta and B atoms in a section of the final three-dimensional (3D) configuration obtained by RMC. Branching and linear B-B chains as well as B-Ta contacts can be observed. It is reasonable to suggest that the network of boron atoms and B-Ta bonds hinder the nucleation of the crystalline phase and, thus, increase the thermal stability of the $Co_{43}Fe_{20}Ta_{5.5}B_{31.5}$ glass.

A number of intrinsic and extrinsic factors are considered to characterize (identify) glass-forming abilities of metallic alloys and thermal stability of glasses.[17–24] Topological and chemical short-range atomic ordering has been suggested to

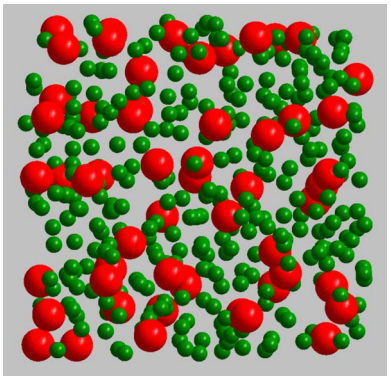

FIG. 5. (Color online) Distribution of Ta (large spheres) and B (small spheres) atoms in the $Co_{43}Fe_{20}Ta_{5.5}B_{31.5}$ metallic glass. A section ($\sim$21.3 Å)^3 of the final 3D configuration box ($\sim$61.2 Å)^3 obtained by RMC. Co and Fe atoms are not shown for clarity.

play a crucial role in the glass formation process. GFA and thermal stability of the CoFeTaB alloy are significantly better as compared either to Co-B and Fe-B binary or Co-Fe-B ternary alloys. Bulk glass is obtained from the four-component melt, while this is not possible in the case of binary or ternary alloys. The crystallization temperature of $Co_{43}Fe_{20}Ta_{5.5}B_{31.5}$ MG increases by 235 K[3] in comparison, for example, with 747 K in the ternary $Co_{71.2}Fe_{5.8}B_{23}$ glass.[25] Our findings show that quaternary CoFeTaB glass is characterized by a strong chemical ordering. The total coordination numbers in the CoFeTaB MG—$\langle N_{Co}\rangle = 14.3 \pm 0.8$, $\langle N_{Fe}\rangle = 13.6 \pm 1.4$, $\langle N_{Ta}\rangle = 15.1 \pm 1.5$, and $\langle N_B\rangle = 9.4 \pm 1.0$—prove a very dense atomic packing, which belongs to the factors supporting GFA. The uncertainties have been estimated by changing systematically the individual N_{ij} values of Table I by applying constraints in the test RMC runs (e.g., N_{CoCo} was forced to be 6.0 instead of 7.0). It has been found that uncertainties largely cancel out at the level of total coordination numbers. It can be assumed that the dense atomic packing and strong interaction between unlike atoms[26] also contribute to the high fracture strength and Young's modulus characteristic for the CoFeTaB glass.

In summary, we have carried out a complex study of the four-component $Co_{43}Fe_{20}Ta_{5.5}B_{31.5}$ metallic glass that allowed us to resolve all ten partial pair distribution functions and determine the topological and chemical short-range atomic order. It is found that each boron atom has an average 2.3 nearest boron neighbors in the $Co_{43}Fe_{20}Ta_{5.5}B_{31.5}$ metallic glass, which is significantly higher than N_{BB} in glassy $Co_{81.5}B_{18.5}$ and $Fe_{80}B_{20}$ and even in $Ni_{65}B_{35}$ ($\sim$1). The existence of Ta-based structural units whose composition is very close to the composition of the $(Co,Fe)_{21}Ta_2B_6$ crystalline phase precipitating upon annealing of the glass is established. The Ta-based structural units might act as the centers for nucleation of this crystalline phase. Dense atomic packing, on one hand, and the appearance of Ta-B and B-B bonds, which are absent in the crystalline state, on the other hand, are suggested to be responsible for the high glass-forming ability, thermal stability, and the mechanical properties of the $Co_{43}Fe_{20}Ta_{5.5}B_{31.5}$ metallic glass.

P.J. was supported by the Hungarian Academy of Sciences and the Hungarian Basic Research Found (OTKA) Grant No. T048580. I.K. acknowledges Deutsches Elektronen-Synchrotron DESY (Hamburg, Germany) for the support of experiments performed at HASYLAB.

*Corresponding author; ivan.kaban@physik.tu-chemnitz.de
†Also at TU Dresden, Institute of Materials Science, D-01062 Dresden, Germany

[1] A. Inoue, B. L. Shen, and C. T. Chang, Intermetallics **14**, 936 (2006).
[2] A. Inoue, B. L. Shen, H. Koshiba, H. Kato, and A. R. Yavari, Nature Mater. **2**, 661 (2003).
[3] A. Inoue, B. L. Shen, H. Koshiba, H. Kato, and A. R. Yavari, Acta Mater. **52**, 1631 (2004).
[4] B. Shen and A. Inoue, J. Phys.: Condens. Matter **17**, 5647 (2005).
[5] B. Shen, S. Pang, T. Zhang, H. Kimura, and A. Inoue, J. Alloys Compd. **460**, L11 (2008).
[6] I. Kaban, S. Gruner, W. Hover, P. Jóvári, R. G. Delaplane, and A. Wannberg, J. Non-Cryst. Solids **353**, 3027 (2007).
[7] P. Jóvári, S. N. Yannopoulos, I. Kaban, A. Kalampounias, I. Lishchynskyy, B. Beuneu, O. Kostadinova, E. Welter, and A. Schöps, J. Chem. Phys. **129**, 214502 (2008).
[8] P. Jóvári, K. Saksl, N. Pryds, B. Lebech, N. P. Bailey, A. Mellergård, R. G. Delaplane, and H. Franz, Phys. Rev. B **76**, 054208 (2007).
[9] P. Jóvári, I. Kaban, J. Steiner, B. Beuneu, A. Schöps, and M. A. Webb, Phys. Rev. B **77**, 035202 (2008).
[10] R. L. McGreevy and L. Pusztai, Mol. Simul. **1**, 359 (1988).
[11] L. Pusztai and E. Sváb, J. Phys.: Condens. Matter **5**, 8815 (1993).
[12] http://webelements.com.
[13] P. Lamparter, E. Nold, G. Rainer-Harbach, E. Grallath, and S. Steeb, Z. Naturforsch. A **36**, 165 (1981).
[14] P. Villars and L. D. Calvert, *Pearson's handbook of crystallographic data for intermetallic phases* (ASM International, Materials Park, Ohio, 1991), Vol. 2.
[15] H. H. Stadelmaier, H. H. Davis, H. K. Manaktala, and E.-T. Henig, Z. Metallkd. **80**, 370 (1989).
[16] A. Westgren, Jernkontorets Ann. **117**, 501 (1933).
[17] J. Hafner, Phys. Rev. B **21**, 406 (1980).
[18] A. Inoue, Acta Mater. **48**, 279 (2000).
[19] J. Z. Jiang, T. J. Zhou, H. Rasmussen, U. Kühn, J. Eckert, and C. Lathe, Appl. Phys. Lett. **77**, 3553 (2000).
[20] T. Egami, J. Non-Cryst. Solids **317**, 30 (2003).
[21] D. B. Miracle, Nature Mater. **3**, 697 (2004).
[22] H. W. Sheng, W. K. Luo, F. M. Alamgir, J. M. Bai, and E. Ma, Nature (London) **439**, 419 (2006).
[23] V. Kokotin and H. Hermann, Acta Mater. **56**, 5058 (2008).
[24] D. V. Louzguine-Luzgin, D. B. Miracle, and A. Inoue, Adv. Eng. Mater. **10**, 1008 (2008).
[25] J. Latuszkiewitcz, T. Kulik, and H. Matyja, J. Mater. Sci. Lett. **15**, 2396 (1980).
[26] F. R. De Boer, R. Boom, W. C. M. Mattens, A. R. Miedema, and A. K. Niessen, *Cohesion in Metals: Transition Metal Alloys* (North-Holland Physics Publishing, Amsterdam, 1989).